ARTICLE NO. 78-1141R

Characteristics of the Near Wake of a Compressor of a Fan Rotor Blade

B. Reynolds,* B. Lakshminarayana,† and A. Ravindranath*
The Pennsylvania State University, University Park, Pa.

Research reported in this paper covers an experimental investigation of the rotor wake. The experimental investigation included a study of the mean velocity, turbulence intensity, and Reynolds stress variations across the wake of a lightly loaded rotor blade at various axial and radial locations. Only the mean velocity data and their interpretation are presented in this paper. Measurements were carried out with a triaxial probe, rotating with the rotor and stationary behind the rotor. Also, measurements were made with a spherical head static pressure probe rotating with the rotor. Wakes were measured at various incidences to discern the effect of blade loading on the rotor wake. The wake is found to be three-dimensional in nature with appreciable radial velocity. The measurements close to the blade trailing edge indicate that the decay of the wake is rapid in this region. The wake data are correlated to derive expressions for the profile and decay of all the components.

Nomenclature

$B_1 \ldots B_6$ = constants defined in Eqs. (4-6)
c = rotor blade chord length
c_d = section drag coefficient
E = mean voltage measured by hot wire
e = fluctuating component of the voltage measured by hot wire
i = incidence of inlet flow with rotor blade in relative (rotating) frame of reference
L_s, L_p = wake width at half the depth on the rotor blade suction (trailing surface and pressure (leading) surface of the wake, respectively)
LS, TS = leading and trailing surfaces of the rotor blade, respectively
p = static pressure
Q = resultant [relative velocity $(\sqrt{U^2+V^2+W^2})$]
R = radius ratio $= r/r_t$; r_t is tip radius and r is the local radius
r, θ, z = rotating cylindrical coordinate system; radial, tangential, and axial, respectively
S = blade spacing
s = streamwise distance
U, V, W = relative mean velocities in radial, tangential, and axial directions, respectively
u, v, w = defect in relative mean velocities in radial, tangential, and axial directions, respectively
u', v', w' = fluctuating component of relative velocities in radial, tangential, and axial directions, respectively
U_r, U_n, U_s = relative velocities in the radial, normal, and streamwise directions, respectively
Y = tangential distance from wake centerline nondimensionalized by blade spacing ($r\theta/S$, $\theta = 0$ at wake centerline)
Z = axial distance from rotor blade row nondimensionalized by chord length of rotor blade
ψ = stagnation pressure rise coefficient
ψ_s = static pressure rise coefficient $(p_2 - p_1)/1/2\rho(Q_2)^2$
Ω = rotor speed of rotation
δ = semiwake width, $(L_s + L_p)$
η_s, η_p = wake traverse direction normalized by L_s and L_p, respectively

Subscripts

c = value at the wake center
d = defect (difference between freestream and wake value)
e = wake edge
m = maximum value in wake
t = tip
0 = freestream value
$1,2$ = inlet and outlet to rotor, respectively

Superscript

$\bar{()}$ = time average

Introduction

THE study of rotor blade wakes is important for establishing improved aerodynamic design criteria, predicting noise levels, and determining the vibration characteristics of turbomachinery used in aircraft, naval, space, and land applications. It is also a source of loss in efficiency. For these reasons, knowledge of rotor or fan wake characteristics is essential for building quieter and more efficient turbomachinery. The knowledge gained through such a study has scientific significance in that it provides information on the effects of rotation and curvature on the development and decay of turbulent shear flows.

A highly three-dimensional flow caused by centrifugal forces, Coriolis forces, and complex blade geometries is characteristic of the rotor wake. Of the limited number of experimental investigations undertaken to date, no systematic data in the near-wake region downstream of the rotor have been collected. It was the basis of this investigation to provide experimental meausrements of the rotor wake in the near-wake region. A review of the experimental investigations of the rotor wake is given by Reynolds.[1]

Received June 12, 1978; presented as Paper 78-1141 at the AIAA 11th Fluid and Plasma Dynamics Conference, Seattle, Wash., July 10-12, 1978; revision received April 9, 1979.

Index categories: Airbreathing Propulsion; Rotating Machinery; Jets, Wakes, and Viscid-Inviscid Flow Interactions.

*Graduate Assistant, Dept. of Aerospace Engineering. Student Member AIAA.

†Professor, Dept. of Aerospace Engineering. Associate Fellow AIAA.

Experimental Equipment and Procedure

Rotor wake measurements were carried out with a triaxial hot-wire probe, rotating with the rotor and stationary behind the rotor. Wakes were measured at varying rotor blade incidences to discern the effect of blade loading on the wake. Using the proceding experimental procedure, the three-dimensional mean velocity and turbulence characteristics were determined in both the near- and far-wake regions. The rotating hot-wire probe wake measurement technique described by Gorton and Lakshminarayana[2] and the stationary hot-wire probe measurement technique reported by Lakshminarayana and Poncet,[3] were used to obtain the experimental results in this paper.

Description of Facility and Operating Conditions

The Axial Flow Research Fan Facility at the Applied Research Laboratory of the Pennsylvania State University was used for all rotor wake measurements made in this investigation. The rotor and traverse mechanism assembly are shown schematically in Fig. 1. At a fixed rotor speed of rotation, operating conditions were varied by adjusting the auxiliary fan in the facility. To remove foreign particles from the flow measured by the triaxial hot-wire probe, a large dust screen was placed around the bellmouth inlet. The axial flow research fan has the following physical dimensions and specifications: overall length = 5.99 m, inner cylindrical casing diameter = 0.546 m, hub diameter = 0.241 m, and rotor motor power (enclosed in hub) = 749.0 kg-cal/min. Rotor revolutions per minute or cycles per second are measured by a photocell attached to the rotor shaft. A detailed description of the facility is given by Bruce.[4]

A 12-bladed (uncambered) rotor was used for all the wake measurements reported in this paper. Each rotor blade section was a British C1 profile with the rotor designed as a free vortex type. The blade chord is 15.2 cm, space chord ratio and stagger angles are 0.68 and 45 deg, respectively, at midradius. The rotor was operated at 1010 rpm with the blades operating at 0, 5, 10, and 15 deg incidences at the midradius. Rotating probe data were recorded at the 0 and 10 deg incidence operating conditions, while stationary hot-wire probe data were recorded at all of the incidences tested. Far-wake data at 0 deg were presented in Ref. 5. Only the mean velocity data at 0 and 10 deg incidences and their interpretation are presented in this paper. The turbulence data and their interpretation will be presented in a later paper.

Rotating Probe Traverse Mechanism

A rotating probe traverse mechanism was designed and built to both rotate the probe with the rotor and enable the probe to be traversed across the wake in the tangential direction while the rotor is in motion. All electrical signals from the triaxial hot wire were transferred to the stationary frame of reference through a mercury slip ring unit.

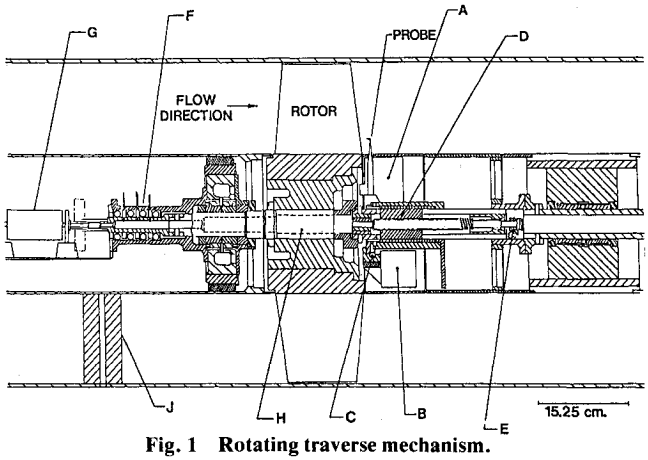

Fig. 1 Rotating traverse mechanism.

Figure 1 shows the important features of the probe traverse mechanism built for use in the axial flow research fan. Two major functions were performed by the mechanism: to allow the probe to be traversed across the wake at a variety of axial and radial locations, and to allow probe signals to be transferred to the stationary frame of reference through the data transmission system illustrated in Fig. 1. Additional references can be found in Refs. 1 and 6.

Probes, Instrumentation, and Data Processing

A triaxial hot-wire probe was used for all velocity measurements made in this investigation. The probe could measure accurately the three-dimensional mean velocity and turbulence characteristics of the rotor wake when used in either the rotating or stationary probe experimental programs.

A spherical head static pressure probe (made by Datametrics) was rotated with the traversing mechanism to measure the static pressure distribution in the wake. This probe was insensitive to large pitch or yaw angles which are encountered in the three-dimensional wake flow being measured.

The rotating hot-wire probe and the instrumentation used are similar to those of Ref. 2 and are described in Ref. 1. Consistent with the data processing assumptions of Ref. 2 ($U_s > U_r > U_n$) the triaxial probe was aligned in an approximate relative streamwise coordinate system. Rotor wake measurements made in Ref. 5, where U_r was everywhere less than 25% of U_s, indicated that the assumption $U_s > U_r > U_n$ should be valid in the present investigation. Near-wake data in the present investigation showed U_r less than 30% of U_s, except at $Z = 0.007$, $i = 0$ deg, in agreement with the data processing assumption. The measurement technique enabled three components of mean velocity, turbulence intensity, and Reynolds stress to be determined.

The stationary probe experimental technique described in Refs. 3 and 5 uses ensemble averaging of the recorded periodic and random unsteadiness of the rotor wake in the stationary frame to determine wake flow properties. For the experimentation reported in this paper, 120 wakes were used for the ensemble average of the triaxial probe measurements with 301 points describing the blade-to-blade variations. A complete description of the stationary probe experimental program, from which the measurements reported in the paper were found, is given in Ref. 1.

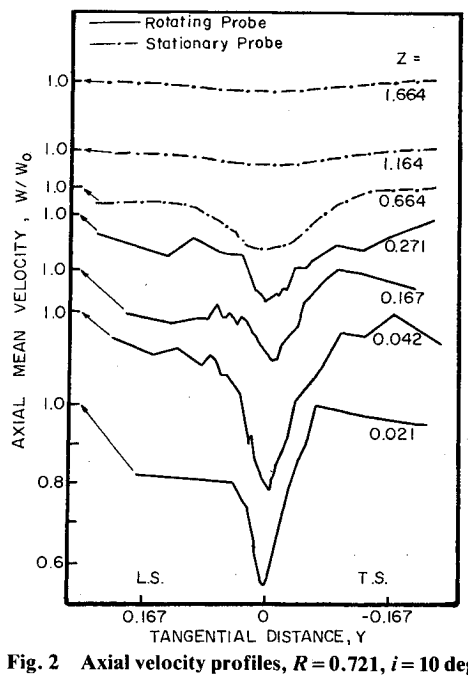

Fig. 2 Axial velocity profiles, $R = 0.721$, $i = 10$ deg.

Experimental Data and Interpretation

Rotating and stationary triaxial hot-wire probe measurements have been used to study the rotor wake in both the near- and far-wake regions. The near wake is defined as the region where the defects are of the same order of magnitude as the freestream velocity. The far-wake defects are small compared to freestream velocity. With these measurements, the mean velocity and turbulence characteristics of the rotor wake were found. A correlation of the wake measurements was found and the similarity rules for mean velocity were examined. Static pressure variations across the rotor wake in the near-wake region were also studied. Only some typical data are presented in this paper. All the data are presented in Ref. 1.

Mean Velocity Profiles

All of the velocities discussed in this section are relative velocities (in the rotating frame of reference) and are normalized, unless otherwise stated, by the freestream axial velocity.

Axial Velocity

Variation of the axial velocity profiles in the rotor wake at midradius ($R=0.721$) with rotor blade incidences of 10 and 0 deg are illustrated in Figs. 2 and 3, respectively. The wake profiles in Fig. 2 clearly show the asymmetry about the wake centerline in the near-wake region. This indicates that the rotor blade suction surface boundary layer is thicker than the pressure surface boundary layer. At the 10 deg incidence operating condition, the trailing surface becomes the suction side of the uncambered rotor blade, while the leading surface is the pressure side. Asymmetry of the wake profiles in Fig. 2 is discernable even at the far-wake station $Z=0.271$, but has become much less pronounced. At the far downstream stations, $Z=1.164$ and $Z=1.664$, the rotor wake has become symmetric about its centerline. Symmetry in the rotor wake profiles results from the wake spreading and mixing with the freestream, as well as interchange of momentum and energy on either side of the wake.

The wake profiles shown in Fig. 3 for the 0-deg operating condition do not exhibit the large asymmetry measured for the 10 deg operating condition. This is expected since the leading and trailing surface boundary layers should be the same for an uncambered rotor blade operating at nearly zero incidence. It should be noted that at the 10 deg operating condition the blade row investigated was operating as a weak turbine, resulting in the slight asymmetry seen in the profiles. No asymmetry is seen in the wake profiles at the far downstream station $Z=0.420$.

At 10 deg incidence (Fig. 2), the axial velocity profiles show a lower value of the freestream velocity on the pressure side and a higher value on the suction side; this is a consequence of the existence of pressure gradients (inviscid effect) across the passage immediately downstream of the trailing edge. This effect decreases beyond $Z=0.042$ (which is .635 cm from the trailing edge for a blade of 15.2 cm chord). At $Z=0.271$, the effect disappears.

In the near-wake region, the wake defect, $1-(W/W_0)$, is seen to be about 0.40 at $Z=0.021$ for 10 deg incidence and 0.32 at $Z=0.032$ for 0 deg incidence. The largest values for wake defects are seen in the trailing-edge and near-wake regions. Far downstream, the wake defect is reduced to 0.035 at $Z=1.664$ for 10 deg incidence and 0.09 at $Z=0.420$ for 0 deg incidence. The maximum defect in axial velocity is higher for 10 deg incidence than for the 10 deg case at all axial locations.

The variation of the tangential gradients of axial mean velocity in the wake indicate the pronounced change in profile shape downstream of the rotor. At Z stations in the near-wake region, at both the 10 and 0 deg operating conditions (Figs. 2 and 3), the gradients are very large. This characteristic results from the development of the flow as it moved through the rotor blade row and in transition from boundary layer to a wake. Spreading of the wake and mixing with the freestream results in a milder velocity gradient in the far-wake region. The steep gradients of velocity in the near wake, especially at the wake center, represents a very unstable flow condition.

Tangential Velocity

The relative tangential velocities are shown plotted in Figs. 4 and 5 at various distances downstream of the blade trailing edge and at 10 and 0 deg incidences, respectively. The maximum defect seems to be slightly larger than the axial velocity defect at both rotor blade incidences. For 10 deg incidence, the initial defect is about 0.64, which reduces to a value of 0.28 at $Z=0.271$. Both the tangential and axial velocity profiles show a rapid decay of the defect from trailing edge to about one-quarter chord downstream, becoming less than 20% of the freestream value.

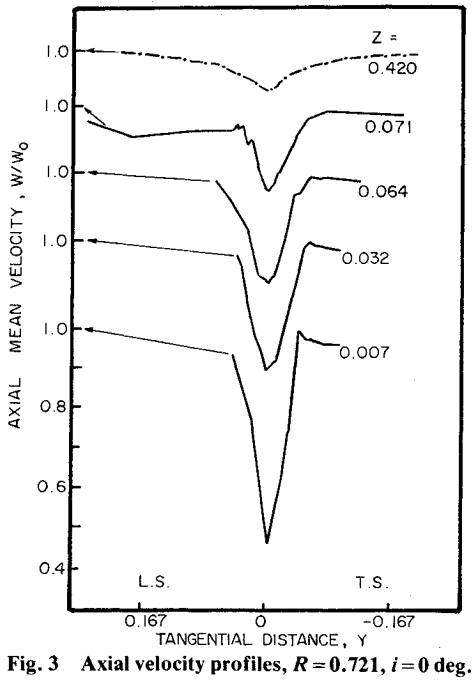

Fig. 3 Axial velocity profiles, $R=0.721$, $i=0$ deg.

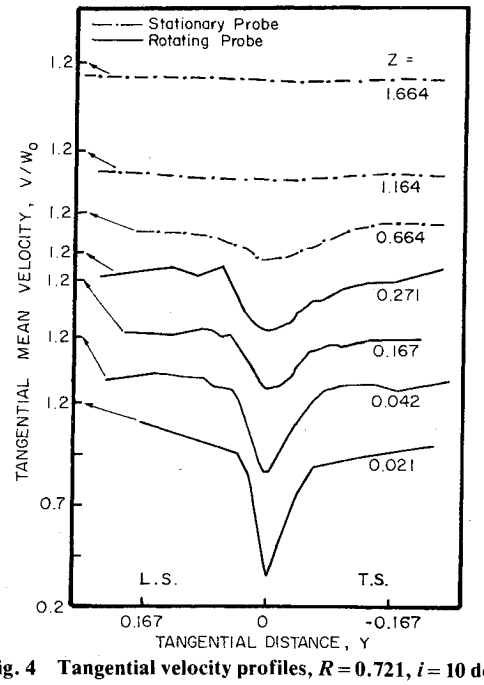

Fig. 4 Tangential velocity profiles, $R=0.721$, $i=10$ deg.

In the near-wake region, the tangential velocity profiles shown in Figs. 4 and 5 are highly asymmetric at the 10 deg incidence operating condition and approximately symmetric for the 0 deg operating condition. As previously discussed, this characteristic results from the boundary-layer developments on the leading and trailing surfaces of the rotor blade.

Similar to the axial velocity profiles in the near-wake region, steep gradients of tangential velocity across the wake were measured in the near-wake region. However, at the far downstream station $Z=1.164$ for $i=10$ deg and $Z=0.420$ for $i=0$ deg the gradients of tangential velocity have disappeared almost completely. This indicates a more rapid decay of relative tangential velocity defect than that for the axial velocity defect in the far-wake regions. It is possible that the rapid decay of tangential velocity defect in the near- and far-wake regions results by an energy exchange from the radial velocities in the wake. Radial velocities partially result from an imbalance between radial pressure gradients and centrifugal forces in the wake. It is through this mechanism that the energy and momentum exchange may take place.

Radial Velocity

Radial velocity profiles at $R=0.721$ (midradius) at incidences of 10 and 0 deg are shown in Figs. 6 and 7, respectively.

Radially outward flows were found to be characteristic of the wake at an incidence of 10 deg. As previously stated, this is caused by an imbalance in the radial pressure gradients and the centrifugal forces. Physically, at either surface of the trailing edge of a compressor or fan rotor blade, the radial velocities must be zero, while the maximum radial velocities occur slightly away from the blade surface. Immediately downstream of the trailing edge, a large redistribution of energy and momentum causes the profile shown at $Z=0.021$ in Fig. 6 to result, with maximum radial velocities at the center of the wake decreasing monotonically toward the outer edge of the wake. The radial velocities in the rotor wake at 10 deg incidence near the trailing edge ($Z=0.021$) are found to be very high. The value at the wake center is about 25% of the axial velocity, but decays rapidly to about 10% at $Z=0.042$. Furthermore, at $Z=0.042$ radial inward velocities are found to exist in the outer regions at the wake. The maximum radial velocity component is seen to decay faster than the axial component for the near-wake region from $Z=0.021$ to $Z=0.042$. Far downstream ($Z=1.164$ and $Z=1.665$), the difference between freestream and wake radial velocities becomes very small.

A very complex flow pattern is evident in the radial velocity profiles shown in Fig. 7 for 0 deg incidence. The maximum radial velocity difference in the wake at $Z=0.071$ has rapidly decayed to about 25% of that measured at $Z=0.007$. Far downstream at about 40% of the blade chord ($Z=0.420$), radial velocities in the wake have decayed to less than 10% of the initial value at $Z=0.007$. While the rotor was operating weakly as a turbine for the 0 deg operating condition, velocity triangles in the wake center are characteristic of a compressor. This effect results in a very unconventional flow pattern. Information defining the radial velocity profiles in the

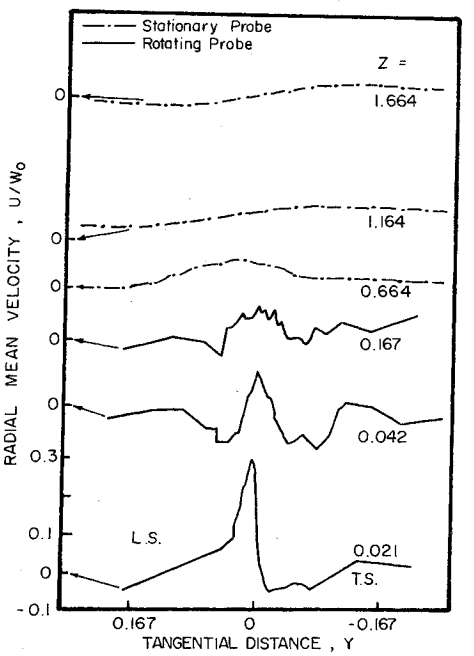

Fig. 6 Radial velocity profiles, $R=0.721$, $i=10$ deg.

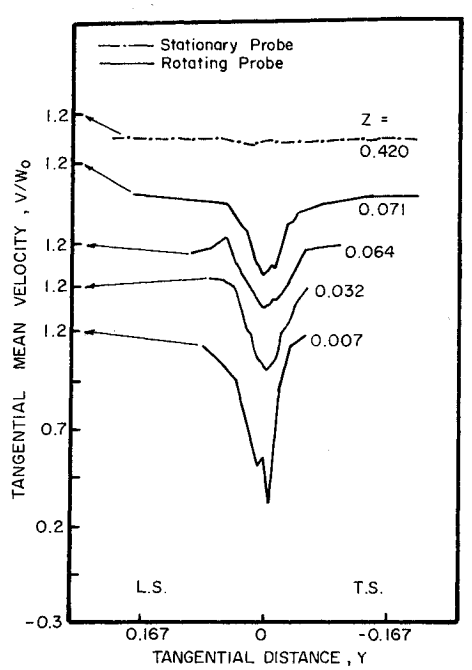

Fig. 5 Tangential velocity profiles, $R=0.721$, $i=0$ deg.

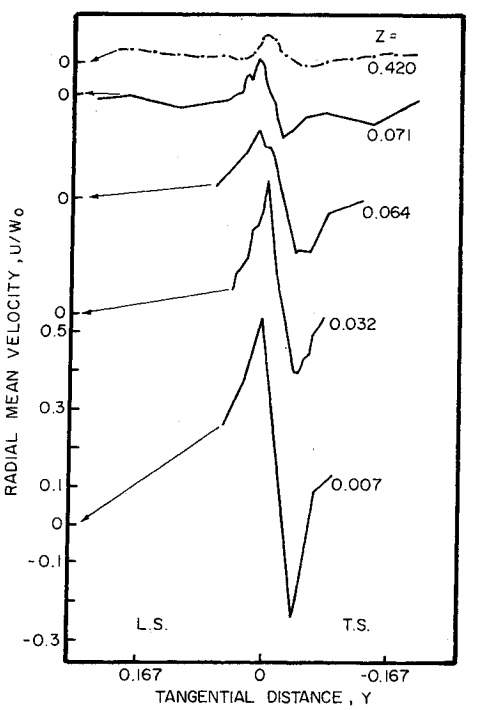

Fig. 7 Radial velocity profiles, $R=0.721$, $i=0$ deg.

boundary layer at the rotor blade trailing edge is not available. For the preceding reasons, no physical explanation of the radial velocity profiles at 0 deg incidence are given in this paper.

In Figs. 6 and 7, the large radial components of mean velocity indicate the highly three-dimensional nature of the rotor or fan wake. The radially inward or outward flow in the wake will result in an increased dissipation of energy and loss in the rotor wake, as compared to the corresponding two-dimensional wake. At a positive blade incidence of 10 deg, a radially outward transport of flow momentum and energy indicates that complex wake behavior can be expected with increasing radius.

Wake Curvature

Curvature of the rotor wake centerline (location of maximum streamwise velocity defect) in the relative frame of reference is shown in Fig. 8 at an incidence of 10 deg for $R=0.721$ (midradius) and $R=0.860$. The curvature of the rotor wake is very small in the near- and far-wake regions at both radial measurement stations. In the near-wake region, the path of the wake centerline is approximately coincident with the rotor blade stagger. The path of the wake centerline is shown to be deflected away from the blade stagger toward the trailing surface of the rotor blade in the far-wake region at about 25% of the chord for $R=0.860$. From momentum and continuity considerations, this can be expected as given by Speidel and Scholz.[7] The deflection of the wake centerline from the stagger angle is appreciable at $R=0.860$.

Similarity in Mean Velocity Profile

Experimental evidence has shown that a similarity in streamwise mean velocity profiles for the wakes behind flat plates, circular cylinders, and isolated airfoils exists. This prompted a search for the similarity in the rotor wake. The similarity rule will be examined for the rotor wake mean velocity measurements reported in this paper.

The maximum velocity difference was used as a non-dimensionalizing velocity scale for all mean velocity profiles. The distance from the wake centerline to the location where the mean velocity defect was half the maximum value was used as a characteristic length scale (L_s and L_p). Using this technique, similarity was found for the axial and tangential mean velocity profiles. The axial velocity similarity profile, shown plotted in Figs. 9 and 10 for 10 and 0 deg incidences, respectively, seem to follow the Gauss' function ($e^{-0.693\eta^2}$). The tangential velocity defect for both rotor blade incidences, shown in Figs. 9 and 10, showed the same trend. Even the radial velocity profiles from measurements made with a positive blade incidence (10 deg incidence) followed this trend (Fig. 11). In Fig. 11, u is the local radial velocity and u_{m_c} is the maximum radial velocity, which in this case occurs at the wake center. No such similarity could be found for the zero incidence case, as the radial velocity distribution is found to be unconventional due to the existence of "compressor" and the "turbine-type" flow behavior within the same wake.

The Gaussian distribution has been derived theoretically for the two-dimensional wake profile from a flat plate. The previous similarity analysis is useful for predicting the rotor wake, using either a theoretically or experimentally derived correlation, such as,

$$q[z,\theta(\text{or }\eta)]=f(z)e^{-0.693\eta^2} \tag{1}$$

where the function q represents one of the mean velocity components in the rotor blade. Attempts are made later to determine the functions $f(z)$ from measurements made in this investigation.

Decay of Radial Velocity and Defects in Axial and Tangential Velocity

Decay of defects in axial and tangential mean velocities at the wake centerline is shown in Fig. 12 at $R=0.721$ for both rotor blade incidences, 0 and 10 deg. Also shown in Fig. 12 are the maximum differences in radial velocity in the wake at 10 deg rotor blade incidence.

A very rapid decay is indicated at the trailing-edge region for both axial and tangential velocity defects at 0 and 10 deg incidences. For the measurements made at both blade incidences, the tangential velocity defect is shown to decay less rapidly than the axial defect in this region. This results in larger tangential components than axial components of mean velocity defect in the near-wake region for both incidences.

At the far downstream measurement stations, $Z=0.42$ at 0 incidence and $Z>1.0$ at 10 deg incidence, axial and tangential

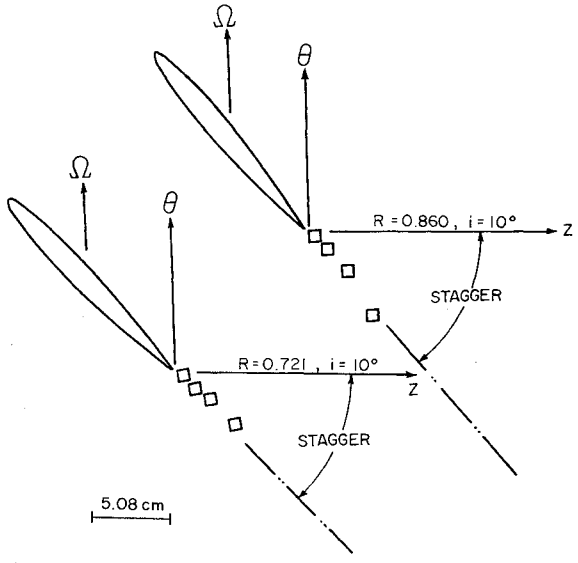

Fig. 8 Curvature of rotor wake centerline at $R=0.721$, $i=10$ deg and $R=0.860$, $i=10$ deg.

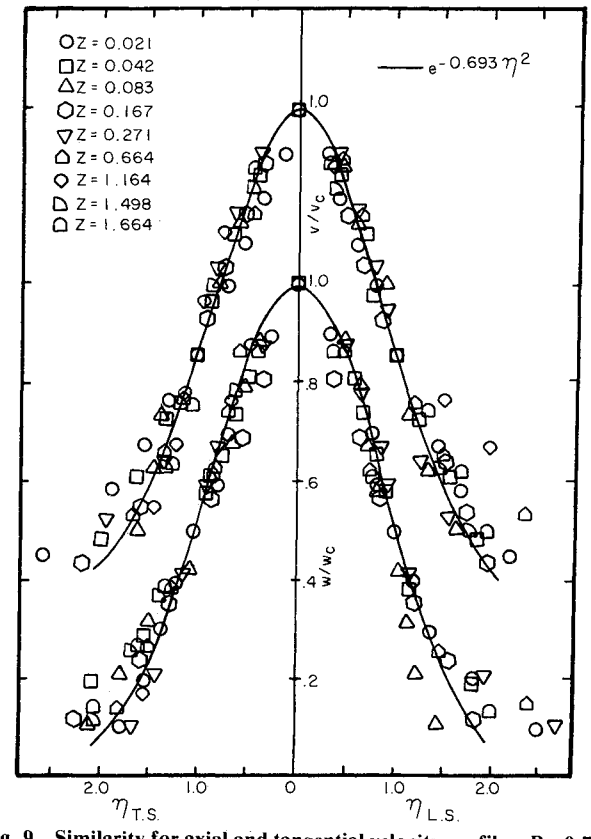

Fig. 9 Similarity for axial and tangential velocity profiles, $R=0.721$, $i=10$ deg.

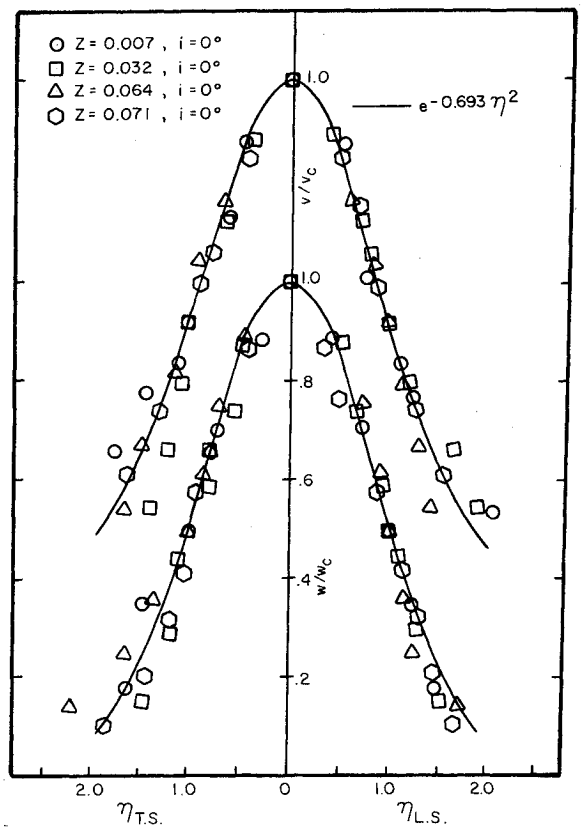

Fig. 10 Similarity for axial and tangential velocity profiles, $R = 0.721$, $i = 0$ deg.

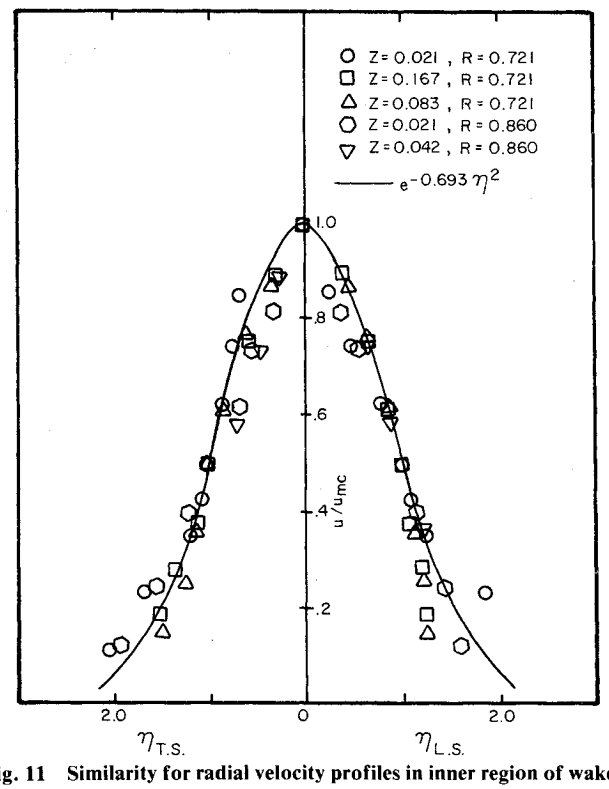

Fig. 11 Similarity for radial velocity profiles in inner region of wake, $i = 10$ deg.

velocity defects have become very small and are decaying very slowly. However, in these regions, the defects in tangential velocity are significantly smaller than the axial defects. This indicates a more rapid decay of tangential defect in the far-wake region than for axial defect. This characteristic is consistent with the results from Lakshminarayana.[8]

Comparison of the near-wake axial and tangential velocity defects for 0 and 10 deg incidence data clearly indicates the effects of blade loading. As shown in Fig. 12, an increase in blade loading increases the defects of both axial and tangential velocities. Although the tangential velocity defect decays slower than the axial component in the trailing-edge region at both blade incidences, this characteristic seems to be most pronounced at 10 deg incidence. Increased blade loading is therefore shown to have a greater effect on tangential velocity defects, more so than for the axial velocity defects.

With the rotor operating at an incidence of 10 deg, a very rapid decay of maximum radial velocity difference is shown in the trailing-edge region. This decay rate slows considerably in the near-wake region. The far-wake region shows a smaller decay rate than that found in the near wake. Maximum radial velocity difference in the wake at the far-downstream measurement stations ($Z > 1.0$) still shows significant radial velocities. Radial velocities in this region are found to increase for increased blade loading. These trends indicate a large radial migration of flow in the rotor wake.

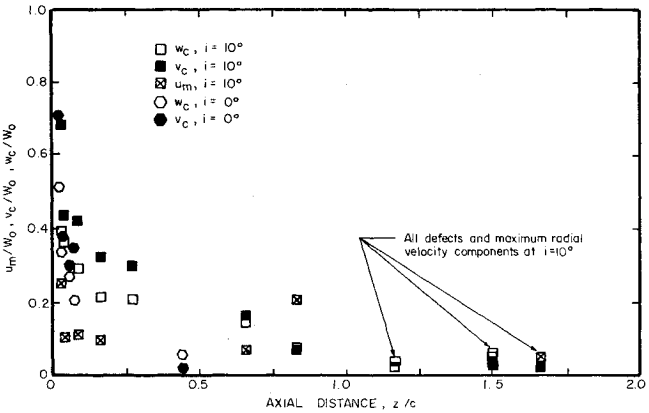

Fig. 12 Decay of radial velocity and defects in axial and tangential velocity at $R = 0.721$ at $i = 0$ and 10 deg.

Decay of Total Mean Velocity

The decay of resultant relative velocity defect is shown in Fig. 13 for measurements made at midradius ($R = 0.721$) at 0 and 10 deg incidence operating conditions. Also shown in Fig. 13 are data from Ref. 9 for measurements made behind an isolated airfoil. The isolated airfoil had a thickness and profile distribution corresponding to the rotor blade sections tested in the present investigation. The effect of increased blade loading is clearly seen for both the isolated airfoil and rotor wake shown in Fig. 13. Increasing incidence is found to slow the decay of total mean velocity. This effect is still discernible for all wake data shown in the far-wake region.

The isolated airfoil wake is shown to decay slower than the rotor wake in the trailing-edge region. Data should be compared for the isolated airfoil and rotor wakes between 0 and 0 deg or between 3 and 10 deg, respectively. The isolated airfoil and rotor blades had identical lift coefficients ($C_l = 0.30$) at the 3 and 10 deg incidences, respectively. In the near-wake region, the isolated airfoil and rotor wakes show similar total velocity defects and decay rates. For measurements in the far-wake region, the rotor wake initially shows a faster decay than the isolated airfoil between $s/c = 1.0$ to $s/c = 1.5$. Beyond $s/c = 1.5$, the rotor wake shows an extremely small decay rate. This may result due to constraints on the rotor wake from adjoining blade wakes. The effect of rotation and centrifugal forces may result in the faster decay rate for the rotor wake in the trailing-edge region than that for the isolated airfoil wake.

Isolated Airfoil, Cascade, and Rotor Wake Correlations

Correlation of the far-wake data behind a body was determined theoretically (Schlichting[10]) using the drag coefficient c_d to collapse mean velocity data from different configurations into a single curve. Schlichting's[10] analysis of the two-dimensional turbulent far wake indicate a dependency of the type,

$$Q_{d_c}/Q_0 = c_d^{1/2} f_1(s/c) \tag{2}$$

However, Silverstein and Katzoff[11] and Silverstein et al.[12] show a good correlation for measurements made behind an isolated airfoil using a different functional dependence for c_d than that given in Eq. (2). This functional dependence was given as:

$$Q_{d_c}/Q_0 = c_d^{1/4} f_2(s/c) \tag{3}$$

Correlated wake defect data have been examined using the relationships given by Eqs. (2) and (3). The correlation given by Eq. (3) has been determined to give better correlation. Hence, correlated isolated airfoil, cascade, and rotor-wake data are presented using the relationship given by Eq. (3).

A correlation of isolated airfoil wake data from Mendelsohn[13] and Preston et al.[14] is shown in Fig. 14 using the functional dependence given by Eq. (3). The correlation seems to work well in the far-wake region ($s/c > 0.25$). Even in the near-wake region, the correlation is quite good. However, in the trailing-edge region the correlation shows a significant degree of scatter. The decay rate in the near-wake region for the isolated airfoil correlation shown in Fig. 14 is found to agree well with the equation given by,

$$\frac{Q_{d_c}}{Q_0} = c_d^{1/4}\left[B_1\left(\frac{s}{c}-\frac{s_0}{c}\right)^{-1/2} + B_2\left(\frac{s}{c}-\frac{s_0}{c}\right)^{-1}\right] \tag{4}$$

where s_0/c represents the virtual origin. The functional relation in Eq. (4) is given by Goldstein[15] for a flat plate laminar wake. This relation is used because no analytical expressions are presently available from a near-wake solution of a turbulent wake. The constants B_1 and B_2 and the virtual origin, determined for the curve shown in Fig. 14, are given in Table 1. The decay rate in the far-wake region agrees well with the curve given by Eq. (4) with $B_2 = 0.0$. This curve is shown in Fig. 14 and the constants and virtual origins are given in Table 1.

A cascade wake correlation is shown in Fig. 14 using the data from Pollard and Gostelow,[16] Lieblein and Roudebush,[17] and Raj and Lakshminarayana.[18] A good correlation is shown in both the near- and far-wake regions using the correlation given by Eq. (3). The functional dependence with s/c is shown in the near- and far-wake regions using the relationship,

$$\frac{Q_{d_c}}{Q_0} = c_d^{1/4}\left[B_3\left(\frac{s}{c}-\frac{s_0}{c}\right)^{-1/2} + B_4\left(\frac{s}{c}-\frac{s_0}{c}\right)^{-1}\right] \tag{5}$$

where $B_4 = 0.0$ in the far-wake region. As in Eq. (4), s_0/c represents the virtual origin. The virtual origins and constants B_3 and B_4 are given in Table 1 for each curve.

Table 1 Constants and virtual origins in Eqs. (4-6)

Equation	Region	Virtual origin, s_0/c	Constants
(4)	Near wake	−0.193	$B_1 = -0.578$, $B_2 = 0.650$
(4)	Far wake	−0.182	$B_1 = 0.495$, $B_2 = 0.0$
(5)	Near wake	−0.141	$B_3 = -0.706$, $B_4 = 0.681$
(5)	Far wake	−0.060	$B_3 = 0.540$, $B_4 = 0.0$
(6)	Near wake	−0.160	$B_5 = -0.361$, $B_6 = 0.463$
(6)	Far wake	−0.360	$B_5 = 0.271$, $B_6 = 0.0$

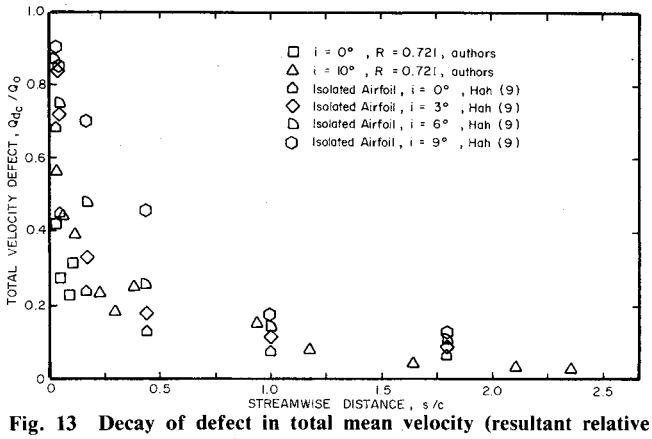

Fig. 13 Decay of defect in total mean velocity (resultant relative velocity) in streamwise direction at wake centerline.

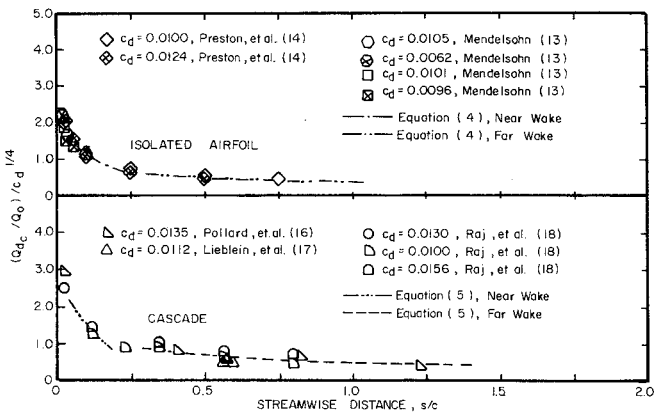

Fig. 14 Correlation for the maximum velocity defect for isolated airfoil and cascade wake.

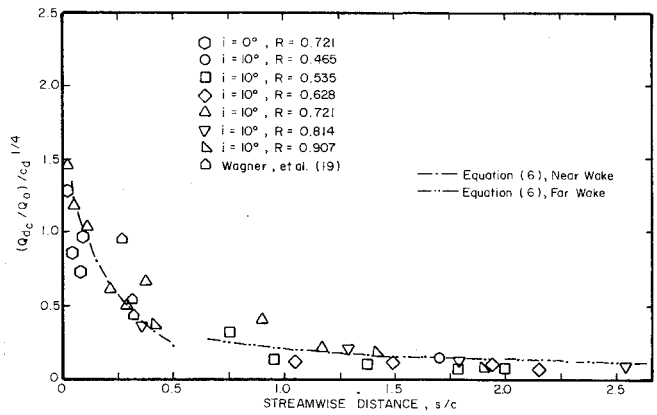

Fig. 15 Correlation of maximum velocity defect for rotor wake.

A rotor wake correlation is shown in Fig. 15 using data from the present investigation and from Wagner et al.[19] The correlation using $c_d^{1/4}$ is shown to be good for both the near- and far-wake regions. However, a larger scatter is shown than that for the isolated airfoil or cascade wake correlations. The correlated data show reasonable agreement with the equation:

$$\frac{Q_{d_c}}{Q_0} = c_d^{1/4}\left[B_5\left(\frac{s}{c}-\frac{s_0}{c}\right)^{-1/2} + B_6\left(\frac{s}{c}-\frac{s_0}{c}\right)^{-1}\right] \tag{6}$$

in both the near- and far-wake regions. The functional dependence with s/c is shown in the far-wake region for $B_6 = 0.0$. Constants B_5 and B_6 and virtual origins for each curve are given in Table 1.

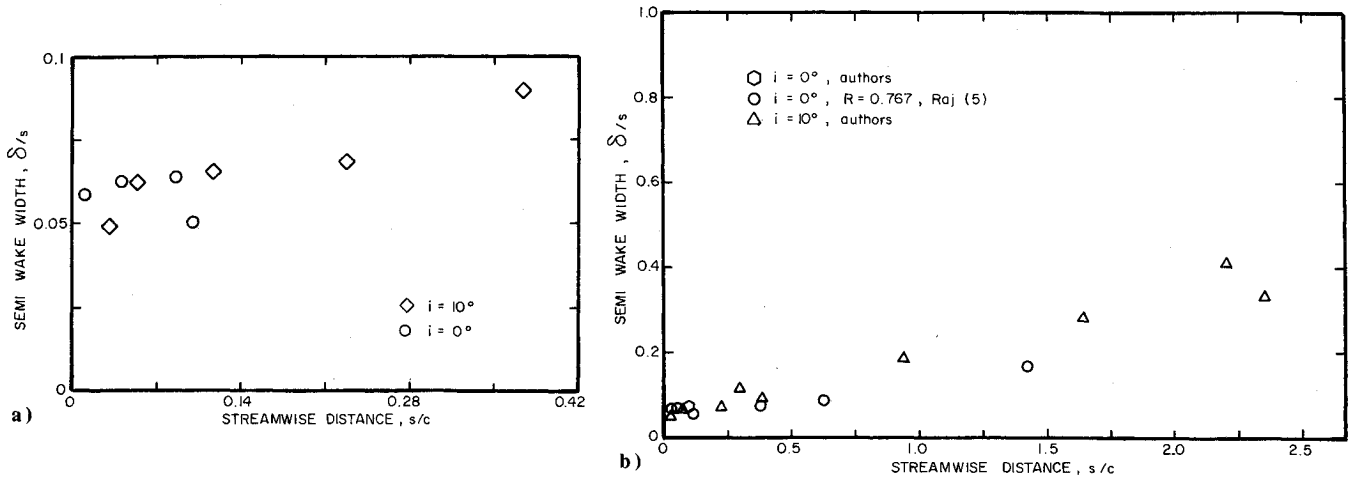

Fig. 16 a)Variation of semiwake-width at midradius (near-wake data). b) Semiwake-width variation downstream of the rotor at $R=0.721$.

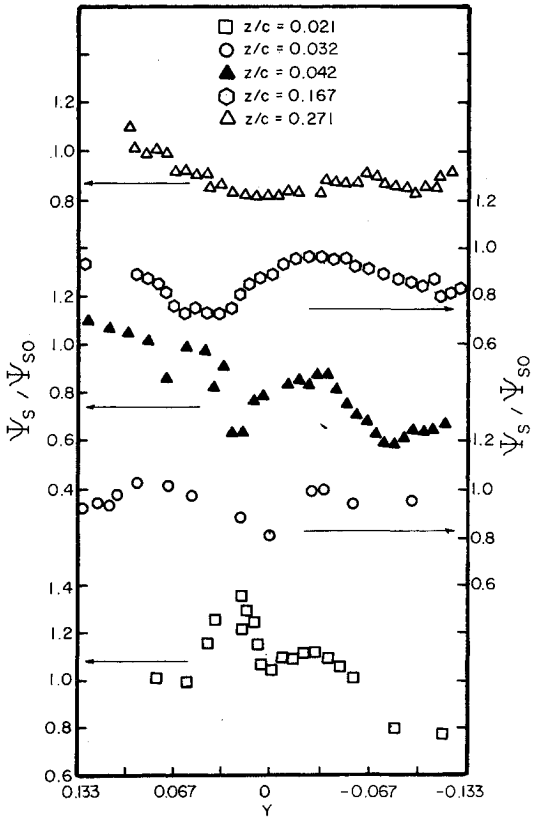

Fig. 17 Static pressure variation in rotor wake.

Wake Width

The variation of semiwake is shown in Fig. 16a for measurements made at midradius ($R=0.721$) with rotor blade incidences of 0 and 10 deg. The data in the near wake are shown in Fig. 15a and all the data in Fig. 16b.

For 10 deg incidence near the trailing-edge region (Fig. 16a), the semiwake width grows rapidly between $s/c=0.030$ and 0.059. Wake width seems to increase at a rate proportional to s/c in this region. In the near-wake region from $s/c=0.059$ to $s/c=0.236$, the wake width is shown to be nearly constant. Wake width is then found to increase again beyond $s/c=0.236$. The variation of semiwake width at 0 incidence shows a similar trend, except for some scatter in the data at $s/c=0.099$. This behavior is contrary to those observed for an isolated airfoil (Preston et al.,[14] Mendelsohn,[13] and Silverstein et al.[12]) and for a flat plate (Chevray and Kovasznay[20]). The effect of three-dimensional flow on the wake can clearly be seen here. The radial transport of mass, momentum, and energy may be responsible for the near-constant wake width at midradius, even though the wake defect is decaying rapidly.

Semiwake width is shown in Fig. 16b for 0 and 10 deg incidences in the far-wake region. Here, semiwake width seems to increase at a rate given by $\sqrt{s/c}$. The effect of increased blade loading is found to increase the wake width in the far-wake region for all measurement stations shown.

The trends observed for the rotor wake near the trailing-edge region for $s/c<0.059$ and in the far-wake region for $s/c>0.236$ seem to be consistent with the results from a single airfoil. In these regions, the functional dependence of semiwake width with s/c was found to be proportional to s/c and $\sqrt{s/c}$ for the trailing-edge and far-wake regions, respectively.

Static Pressure Distribution

The static pressure distribution across the rotor wake at midradius and at an incidence 10 deg is shown in Fig. 17. The static pressure data show an appreciable variation of static pressures inside the wake as well as in the inviscid freestream. Thompkins and Kerrebrock[21] have also reported 20-25% variations in static pressure at 10% of the axial chord downstream of a transonic rotor. These data seem to confirm the trends described previously for the present investigation.

At $Z=0.021$, the static pressure variation in the wake is about 25%. The variation of static pressure in the wake is reduced substantially at about ¼ chord ($Z=0.271$). This characteristic of the static pressure profiles seem to justify some of the assumptions made in the far-wake analysis of Ref. 8. However, one must view the static pressure data with caution. There are spatial errors, as well as large turbulence intensities in the wake flow measured, and this may introduce errors in the data.

Conclusions

The measurements reported in this paper represent the first data in the near-wake region of a rotor blade from a rotating triaxial probe. The major conclusions derived on the basis of rotor wake measurements presented in this paper are:

1) Radial, tangential, and axial velocity defects in the rotor wake decay very rapidly in the trailing-edge region. This rate is substantially reduced in the near-wake region.

2) Large radial velocities in the near-wake region indicate a large radial migration of momentum and energy. This characteristic will alter the rotor wake properties when compared to a corresponding two-dimensional wake.

3) The tangential velocity defect decays slower than the axial velocity defect in the trailing-edge region.

4) Increased blade loading slows the decay rates of tangential and axial velocity defects.

5) The rotor wake showed a good correlation with $c_d^{1/4}$ in the near- and far-wake regions.

6) The behavior of the growth of the wake width is quite different from that for a two-dimensional wake.

Acknowledgment

This work was supported by National Aeronautics and Space Administration through Grant NSG 3012 with M. F. Heidmann as the technical monitor. Grateful acknowledgment is made to G. Sayers, G. B. Gurney, and R. Raj for the design of the rotating probe traverse mechanism, and to J. Rishell, W. Nuss, and E. Jordan for their aid in the instrumentation setup.

References

[1] Reynolds, B. D., "Characteristics of Lightly Loaded Fan Rotor Blade Wakes," M.S. Thesis, Dept. of Aerospace Engineering, The Pennsylvania State University, Nov. 1978.

[2] Gorton, C. A. and Lakshminarayana, B., "A Method of Measuring the Three-Dimensional Mean Flow and Turbulence Quantities Inside a Rotating Turbomachinery Passage," *Journal of Engineering for Power*, Vol. 98, No. 2, April 1976, pp. 137-146.

[3] Lakshminarayana, B. and Poncet, A., "A Method of Measuring Three-Dimensional Rotating Wakes Behind Turbomachinery Rotors," *Journal of Fluids Engineering*, Vol. 96, No. 4, June 1974, pp. 87-91.

[4] Bruce, E. P., "The ARL Axial Flow Research Fan—A New Facility for Investigation of Time-Dependent Turbomachinery Flows," ASME Paper 74-FE-27, Montreal, Canada, May 1974.

[5] Raj, R. and Lakshminarayana, B., "Three-Dimensional Characteristics of Turbulent Wakes Behind Rotors of Axial Flow Turbomachinery," *Journal of Engineering for Power*, Vol. 98, April 1976, pp. 218-228.

[6] Raj, R. and Lakshminarayana, B., "On the Investigation of Cascade and Turbomachinery Rotor Wake Characteristics," NASA CR 134680, 1974.

[7] Speidel, L. and Scholz, N., "Untersuchungen Uber Die Stromungsverluste in Ebenen Schaufelgittern," VDI-Forschungsheft No. 464, 1957.

[8] Lakshminarayana, B., "The Nature of Flow Distortions Caused by Rotor Blade Wakes," AGARD GP-177, 1975.

[9] Hah, C. and Lakshminarayana, B., "Characteristics of an Airfoil Wake," 1979 (in preparation).

[10] Schlichting, H., *Boundary Layer Theory*, McGraw-Hill, Inc., New York, 1968, pp. 685-686.

[11] Silverstein, A. and Katzoff, S., "Design Charts for Predicting Downwash Angles and Wake Characteristics Behind Plain and Flapped Wings," NACA Report No. 648, 1939.

[12] Silverstein, A., Katzoff, W. and Bullivant, W. K., "Downwash and Wake Behind Plain Airfoils," NACA Report No. 651, 1939.

[13] Mendelsohn, R. A., "Wind Tunnel Investigation of the Boundary Layer and Wake and Their Relation to Airfoil Characteristics—NACA 65-012 Airfoil With a True Contour Flap and a Beveled Trailing Edge Flap," NACA TN No. 1304, 1947.

[14] Preston, J. H., Sweeting, N. E., and Cox, D. K., "The Experimental Determination of the Boundary Layer and Wake Characteristics of a Piercy 1240 Aerofoil, with Particular Reference to the Trailing Edge Region," Great Britan Aero. Research Council, R. and M. No. 2031, 1945.

[15] Goldstein, S., "On the Two-Dimensional Steady Flow of a Viscous Fluid Behind a Solid Body," Appendix by A. Fage, *Proceedings of the Royal Society*, London, Vol. 142, 1953.

[16] Pollard, C. and Gostelow, J. P., "Some Experiments at Low Speed on Compressor Cascades," *Journal of Engineering for Power, Transactions ASME*, July 1967, pp. 427-436.

[17] Lieblein, S. and Roudebush, W. H., "Low-Speed Wake Characteristics of Two-Dimensional Cascade and Isolated Airfoil Sections," NACA TN 3771, 1956.

[18] Raj, R. and Lakshminarayana, B., "Characteristics of the Wake Behind a Cascade of Airfoils," *Journal of Fluid Mechanics*, Vol. 61, Pt. 4, 1973, pp. 707-730.

[19] Wagner, J. H., Okiishi, T. H., and Holbrook, G. J., "Periodically Unsteady Flow in an Imbedded Stage of a Multistage, Axial-Flow Turbomachine," ASME Paper 78-GT-6, London, England, April 1978.

[20] Chevray, R. and Kovasznay, S. G., "Turbulence Measurements in the Wake of a Thin Flat Plate," *AIAA Journal*, Vol. 7, Aug. 1969, pp. 1641-1643.

[21] Thompkins, W. T. and Kerrebrock, J. L., "Exit Flow From a Transonic Compressor Rotor," AGARD CP 177, 1975, p. 6-1.